BMP4 expression in the adult rat brain

BMP4 expression in the adult rat brain

SUMIKO MIKAWA,[1] CONG WANG,[1] and KOHJI SATO[1]

[1]Department of Anatomy & Neuroscience, Hamamatsu University School of Medicine, 1-20-1 Handayama, Hamamatsu, Shizuoka 431-3192, Japan

Abbreviated title: BMP4 in the adult brain
Name of Associate Editor: Prof. John L. R. Rubenstein
Index terms: dendrite, neuropil, immunohistochemistry,
Correspondence should be addressed to Kohji Sato.
Department of Anatomy & Neuroscience
Hamamatsu University School of Medicine
1-20-1 Handayama, Hamamatsu,
Shizuoka 431-3192, Japan
Tel & Fax: 81(Japan)-53-435-2288
E-mail: ksato@hama-med.ac.jp
Grant sponsor: the Ministry of Education, Science and Culture of Japan

Abstract

Bone morphogenetic protein-4 (BMP4) is a member of the transforming growth factor β (TGF- β) superfamily and plays important roles in multiple biological events. Although BMP4 expression has been well described in the early development of central nervous system (CNS), little information is available for its expression in the adult CNS. We, thus, investigated BMP4 expression in the adult rat CNS using immunohistochemistry. BMP4 is intensely expressed in most neurons and their dendrites. In addition, intense BMP4 expression was also observed in the neuropil of the gray matters where high plasticity is reported, such as the molecular layer of the cerebellum and the superficial layer of the superior colliculus. Furthermore, we found that astrocytes also express BMP4 protein. These data indicate that BMP4 is more widely expressed throughout the adult CNS than previously reported, and its continued abundant expression in the adult brain strongly supports the idea that BMP4 plays pivotal roles also in the adult brain.

Bone morphogenetic protein-4 (BMP4) is a member of the transforming growth factor β (TGF- β) superfamily (Hogan, 1996). BMP4 signaling has been shown to play an important role in multiple biological events, including neural induction (Harland, 2000), tissue patterning (McMahon et al., 1998), epithelial-mesenchymal interactions underlying organogenesis (Kulessa et al., 2000), lineage selection (Mabie et al., 1999), and in the creation of stem cell “niches” in developing and adult organs (Lim et al., 2000; Watt and Hogan, 2000). BMP4 is synthesized as a large precursor, and subsequently cleaved to yield a carboxy-terminal mature protein. BMP4 exerts its biological functions by interacting with membrane bound receptors belonging to the serine/threonine kinase family including bone morphogenetic protein receptor I (BMPRIA, BMPRIB) and type II (BMPRII) (Sasai and Robertis, 1997). These receptors form heteromeric complexes of type I and type II receptors in which type II is the ligand binding subunit which phosphorylates type I resulting in intracellular cascade events. The functions of BMP4 are also regulated in the extracellular space by secreted antagonistic regulators such as noggin, chordin, follistatin, neurogenesin-1, which are thought to bind BMP4 and prevent their interaction with their receptors (Cho and Blitz, 1998; Ueki et al., 2003).

Also in the developing central nervous system (CNS), BMP4 has been reported to be involved in many pivotal events. For example, in the chick embryo, BMP4 is expressed selectively in the dorsal regions of the odd-numbered rhombomeres (r3 and r5) and induces segmental apoptosis of these regions (Graham et al., 1994). In addition, BMP4 is implicated in repression of the oligodendroglial lineage and generation of the astroglial lineage during brain maturation (Gross et al., 1996; Mabie et al., 1997). However, in the adult CNS, although Lim et al. (2000) have reported that in the adult subventricular zone BMP4 expressed in the type B/C cells potently inhibits neurogenesis, and its antagonist noggin secreted from the ependymal cells makes a niche for adult neurogenesis, the other functions are largely unknown.

BMP4 expression has been well described in the early development of CNS (Jones et al., 1991; Graham et al., 1994; Furuta et al., 1997; Crossley et al., 2001). However, little information is available for BMP4 expression in the adult CNS. Although some reports delineate its expression in the adult CNS (Fan et al., 2003; Charytonick et al., 2000; Peretto et al., 2002; Lim et al., 2000), the reports mainly deal with its expressions in restricted areas. In addition, they are sometimes very contradictory. Furthermore, BMP4 receptors, such as BMPRIA and BMPRII, have been also reported to be abundantly expressed in the adult rat brain (Charytoniuk et al. 2000; Zhang et al. 1998). It is, thus, necessary to perform more wide and detailed investigations of the expression pattern of BMP4 in the adult rat brain. In the present study, we show that BMP4 is more widely expressed than previously reported, and that BMP4 is expressed in neurons and astrocytes.

MATERIALS AND METHODS

Animals and section preparation

Under deep diethylether anesthesia brain samples were isolated from 7 weeks old Wistar rats. For immunohistochemistry, the rats were perfused transcardially with saline followed by 0.1 M phosphate buffer (PB, pH 7.4) containing 4% paraformaldehyde and 0.2% picric acid. The brains were removed rapidly, postfixed in the same fixative for 2 hr at 4 °C. All brains were immersed in 30% buffered sucrose for overnight at 4 °C. Frozen sections (20 μm in thickness) were cut on a cryostat. All experiments conformed to the Guidelines for Animal Experimentation at Hamamatsu University School of Medicine on the ethical use of animals.

Immunohistochemistry

For immunoperoxidase staining, the sections were treated with 10 % normal goat serum, 2 % bovine serum albumin (BSA) and 0.2 % Triton X-100 in 0.1 M PB for 2 hr at room temperature, and incubated further in a monoclonal mouse anti-BMP4 (1:100 dilution; NCL-BMP4, Novocastra, Newcastle, UK) for overnight at 4 °C. The antigen used to produce this antibody is the recombinant mouse bone morphogenetic protein 4. After washing with 0.1 M PB, sections were incubated in goat anti-mouse IgG with peroxidase complex (Histofine Simple Stain Rat MAX-PO; Nichirei, Tokyo, Japan) for 2 hr at room temperature. After washing with 0.1 M PB, immunoreaction was visualized with 3,3’-diaminobenzidine (DAB) (Wako, Osaka, Japan). For double immunofluorescence, sections were treated with 10 % normal chicken serum, 2% BSA and 0.2 % Triton X-100 in 0.1 M PB for 2 hr at room temperature, and incubated further in mouse anti-BMP4 antibody (1:20; Novocastra) and goat anti-GFAP antibody (1:50; Santa Cruz Biotechnology). After washing with 0.1 M PB, sections were incubated in Alexa Fluor 594 chicken anti-mouse IgG (1:500; Molecular Probes, Eugene USA) and Alexa Fluo 488 chicken anti-goat IgG (1:500; Molecular Probes) for 1.5 hr at room temperature. For pre-absorption controls, 1 nmol BMP-4

protein (R&D Systems, Inc., Minneapolis, USA) was added to the diluted primary antisrum (1: 100). Bright-field images were obtained using a microscope (Vanox-AHBS3, Olympus, Tokyo, Japan) equipped with a CCD camera (DP20, Olympus, Japan). Fluorescence images were obtained using a microscope (Eclipse E-600, Nikon, Tokyo, Japan) equipped with a CCD camera (Microfire, Optronics, Goleta, USA). They were further processed using an image analyzing soft (Photoshop, Adobe, Tokyo, Japan).

In situ hybridization

Male adult wistar rats (n=3) were decapitated under diethylether anesthesia. The fresh brains were quickly removed and immediately frozen on powdered dry ice. Serial sections (20 μm thick) were cut on a cryostat, thaw-mounted onto silan-coated slides, and stored at –80 °C. After being warmed to room temperature, slide-mounted sections were fixed in 4% paraformaldehyde in 0.1 M PB (pH 7.2) for 15 min (all steps were performed at room temperature unless otherwise indicated), rinsed three times (5 min each) in 4x SSC (pH 7.2) (1x SSC contains 0.15 M sodium chloride and 0.015 M sodium citrate), and dehydrated through a graded ethanol series (70-100%). The sections were then defatted with chloroform for 5 min, and immersed in 100% ethanol (twice for 5 min each time) before being subjected to hybridization. An antisense oligo cDNA probe for BMP4 mRNA was designed based on the rat BMP4 sequence (ACTGGATCGCTGCAGGCTCCAGACGGTTTGGACGAG). The probe was labeled at the 3' end using [^{35}S]dATP (1000-1500 Ci/mmol (37-55.5 TBq/mmol), New England Nuclear, Boston, MA, USA) and terminal deoxynucleotidyl transferase (Takara, Tokyo, Japan) to obtain a specific activity of approximately 1.4-2.0 x 10^9 d.p.m./μg. Hybridization was performed by incubating the sections with a buffer (4x SSC, 50% deionized formamide, 0.12 M PB (pH 7.2), Denhardt's solution (Nakarai, Kyoto, Japan), 2.5 % tRNA (Roche, Tokyo, Japan), 10% dextran sulfate (Sigma, Tokyo, Japan))containing [^{35}S]dATP (1000-1500 Ci/mmol (37-55.5

TBq/mmol), New England Nuclear, Boston, MA, USA)-labeled probes (1-2 x 10^7 dpm/ml, 0.2 ml/ slides) for 24 h at 41 °C. After hybridization, the sections were rinsed in 1x SSC (pH 7.2) for 10 min, followed by rinsing three times in 1x SSC at 55 °C for 20 min each time. The sections were then dehydrated through a graded ethanol series (70%-100%). After film exposure for 3 days at room temperature, the sections were coated with Kodak NBT-2 emulsion (Kodak, Rochester, NY, USA) diluted 1:1 with water. The sections were then exposed at 4 °C for 4 weeks in a tightly sealed dark box. After being developed in D-19 developer (Kodak), fixed with photographic fixer, and washed with tap water, the sections were counterstained with thionin solution to allow morphological identification. Images were obtained using a microscope (Eclipse E-400, Nikon, Tokyo, Japan) equipped with a CCD camera (Microfire, Optronics, Goleta, USA), and further processed using an image analyzing soft (Photoshop, Adobe, Tokyo, Japan).

Western blotting

Rat cerebral cortex was homogenized in a 50 mM Tris-HCl (pH 7.4) buffer containing protease inhibitor cocktail (Nakarai Tesque, Kyoto, Japan) to avoid degradation of proteins, and solubilized by adding 4 x SDS-PAGE sample buffer containing 4 % 2-mercaptoethanol. After gentle sonication, SDS-PAGE (12.5 % acrylamide) was performed, and proteins were transferred to PVDF membrane (Immobilon-P; Millipore, Billerica, USA) by electroblotting (40 V overnight at 4 ℃) using a transfer buffer (10 mM MOPS, 4 mM sodium acetate [pH 7.5], 20 % ethanol, 0.1 % SDS). Blots were blocked with 5 % BSA in 50 mM Tris-buffered saline containing 0.05 % Tween-20 (TTBS) for 2 hr at room temperature and then incubated with mouse monoclonal anti-BMP4 antiboby (1:200; Novocastra) in TTBS containing 1% BSA. After washing with TTBS, blots were incubated with horseradish peroxidase-linked sheep anti-mouse Ig (1:1500; Amersham Bioscience, Piscataway, USA). Following several washes with TTBS, signals were detected with an ECL western blotting detection kit (Amersham

Bioscience).

ELISA

Solutions of 4 μg/ml of the antigen (BMP4; R&D Systems, Inc., Minneapolis, USA and BMP2; PeproTech EC, London, UK) in 0.1M carbonate buffer (pH9.6) were prepared, 50 μl of the antigen solutions were added to each well (96 Well EIA/RIA Plate; Corning Incorporated, Corning, USA), and then were incubated for overnight at 4℃. After washing the plate with 0.01M PBS, the wells were filled with 3% BSA in 0.1M carbonate buffer, and then were incubated for overnight at room temperature. After washing the plate three times with 0.01M PBS, 50 μl of anti-BMP4 antibody (1:100–1:3200) were added to each well, and then were incubated for 2 hr at room temperature. After washing the plate three times with 0.01M PBS, 50 μl of horseradish peroxidase conjugated sheep anti-mouse Ig (1:4000; Amersham Bioscience Corp., Piscataway, USA) were added to each well, and then were incubated for 2 hr at room temperature. After washing the plate three times with 0.01M PBS, 100 μl of ABTS substrate solution (Roche Applied Science, Basel, Switzerland) were added to each well, and then were incubated for 30 min at room temperature. To quantitate the binding, the results were read at 405 nm using the microplate reader.

RESULTS

Since the amino acid sequences of BMP4 and BMP2 are very similar, we first investigated whether the antibody (NCL-BMP4) can discriminate between them using ELISA method. As shown in Fig. 1A and B, the antibody could specifically recognize only BMP4 protein in a dose-dependent manner. In addition, western blotting with the antibody exhibited a single band of about 19 kD, the size consistent with a previous report (Wozney, 1989; Fig. 1C). Furthermore, pre-absorption of the antiserum with BMP4 completely abolished the immunostaining (Fig. 1D and E). These data indicate that the antibody specifically recognizes BMP4 protein. Finally, we also performed in situ hybridization to detect BMP4 mRNA, and compared the gene expression with the protein expression. As shown in Fig. 1F and G, in both procedures, we found intense reactions in the cerebral cortex and hippocampus. Also in several other regions, BMP4 gene expression and BMP4 protein expression were generally identical (data not shown), further supporting the specificity of the antibody.

General expression patterns

Fig. 2 shows the overview of BMP4 expression in the adult rat brain. BMP4-like immunoreactivity (IR) was observed throughout the adult rat CNS. Abundant BMP4-IR was seen in the olfactory bulb (Fig. 2A), anterior olfactory nucleus (Fig. 2B), basal ganglia (Fig. 2C and D), cortex (Fig. 2B-H), hippocampus (Fig. 2E-G), thalamus (Fig. 2E-G), hypothalamic regions (Fig. 2D-G), midbrain (Fig. 2H), cerebellum (Fig. 2I), brainstem (Fig. 2I and J), and spinal cord (Fig. 2K). In general, gray matters exhibited intense BMP4-IR, in contrast white matters such as the corpus callosum (Fig. 2C-G), internal capsule (Fig. 2E), and fimbura hippocampi (Fig. 2E), showed weak staining. The relative intensity of BMP4-IR in major regions of the rat central nervous system is summarized in Table 1.

Telencephalon

Olfactory bulb

Very strong BMP4-IR was observed in the olfactory nerve layer and external plexiform layer (Fig. 3A). Moderate IR was seen in the other layers including the subependymal layer (Fig. 3A). Closer observation showed that BMP4-IR was detected not only in the neuropil but also in many fibers in the external plexiform layer (arrowheads in Fig. 3B). Based on their appearances, they seemed to be apical dendrites of mitral cells and tufted cells. In addition, cell bodies of mitral cells were also stained (arrows in Fig. 3B).

The septum and nuclei of the diagonal band of Broca

In the lateral septal nucleus, moderate BMP4-IR was detected (Fig. 2C). In the medial septal nucleus, as shown in Fig. 3C, strong positive neurons and patchy neuropil staining were observed. The diagonal band of Broca also exhibited intense BMP4-IR (Fig. 2C).

Piriform cortex

In the layer I of the piriform cortex, very strong BMP4-IR was seen in the neuropil (Fig. 3D). In the layers II and III, many pyramidal neurons were intensely stained with this antibody, and their dendrites were also intensely stained (arrowheads in Fig. 3D).

Cerebral cortex.

Abundant BMP4-IR was detected in the layers I-VI of the cerebral cortex (Fig. 3E). In the layer I, where apical dendrites of pyramidal neurons make synapses with short-axon cells, we observed very strong BMP4-IR in the terminals of apical dendrites and neuropil (Fig. 3F). In the layer V, large pyramidal neurons and their apical dendrites were very intensely stained (arrowheads in Fig. 3G). Fig. 3H shows that many cells in the layer VI were stained with the antibody. The neuropil staining in the layer VI was intenser than that in the corpus callosum (Fig. 3H).

Hippocampus

BMP4-IR was observed throughout the hippocampus (Fig. 4A). The dentate gyrus exhibited relative intenser staining. In the stratum oriens of the Ammon's horn, BMP4-IR was seen in the neuropil, in addition some cells are also immunoreactive (Fig. 4B and C). In the stratum pyramidale, many pyramidal cell bodies exhibited very intense BMP4-IR (Fig. 4B and C). In the stratum radiatum and lacunosum-moleculare, many apical dendrites of pyramidal cells were very strongly stained (arrowheads in Fig. 4C). In the dentate gyrus, intense neuropil staining was observed in the molecular layer (Fig. 4D). In the granular cell layer, most granule neurons showed strong BMP4-IR, in addition BMP4-IR was observed also in the neuropil (Fig. 4E). In the polymorphological layer, neuropil staining was relative weak, while many immunoreactive neurons were scattered (arrowheads in Fig. 4E).

The amygdala and bed nucleus of the stria terminalis

Abundant neuropil staining and cell body staining were also observed in these regions (Fig. 2D-F). Fig. 4F shows many BMP4-IR positive neurons with immnunoreactive dendrites in the basolateral amygdala nucleus (arrowheads in Fig. 4F).

Basal ganglia

The caudate putamen showed strong neuropil staining, and medium sized neurons were also very intensely stained (Fig. 4G). In the globus pallidus, many spindle-shaped neurons were intensely stained, while staining in the neuropil was weak (Fig. 4H). The accumbens nucleus also showed moderate staining (Fig. 2C).

Corpus callosum

In the corpus callosum, small cell bodies were intensely stained (Fig. 4I). On the basis of their appearance, they seemed to be astrocytes.

Diencephalon

BMP4-IR positive cells and neuropil staining were detected in all nuclei in the thalamus (Fig. 2E and F). Fig. 5A and B show BMP4-IR in the anterodorsal nucleus and ventroposterior nucleus. In the both nuclei, abundant cell body staining and moderate neuropil staining were observed. The supraoptic nucleus showed intense cell body staining and neuropil staining (Fig. 5C). The medial preoptic nucleus showed intense BMP4-IR (Fig. 2D). The other hypothalamic nuclei, including ventromedial hypothalamic nucleus (Fig. 2E), arcuate nucleus (Fig. 2F), and mammillary body (Fig. 2G), also showed abundant BMP4-IR.

Midbrain

In the red nucleus, large-sized neurons showed intense BMP4-IR, while neuropil staining was weak (arrowheads in Fig. 5D). The substantia nigra showed strong cell staining and moderate neuropil staining. Fig. 5E shows that dopaminergic neurons in the pars compacta of the substantia nigra exhibited intense BMP4-IR (arrowheads in Fig. 5E). The central gray showed strong neuropil staining (Fig. 2H).

Pons and medulla

Motor system

The nuclei belonging to the general somatomotor and brachiomotor system, such as the motor trigeminal nucleus (Fig. 5F), facial nucleus (Fig. 5G), hypoglossal nucleus (Fig. 5H), ambiguus nucleus (Fig. 5I), showed very intense BMP4-IR. The cell bodies of large motor neurons were very strongly stained, and their BMP4-IR positive dendrites exhibited reticular patterns.

General somatosensory system

In the mesencephalic trigeminal nucleus, large primary afferent neurons were intensely stained (arrowheads in Fig. 5J). In the trigeminal spinal nucleus, many neurons were strongly stained and moderate neuropil staining

was also observed (Fig. 5K). Abundant BMP4-IR was observed in the gracile nucleus, and cuneate nucleus. Fig. 6A shows that neurons in the external cuneate nucleus exhibited very intense BMP4-IR.

Special somatosensory system

Auditory system: The dorsal cochlear nucleus showed abundant BMP4-IR in the neuropil and cell bodies (Fig. 6B). Especially, in the superficial layer of the dorsal choclear nucleus, very intense neuropil staining was observed (Fig. 6B), while in the ventral cochlear nucleus, although intensely labeled neurons were scattered, neuropil staining was weak (Fig. 6C). In the nucleus of the trapezoid body (Fig. 6D), superior olivary complex (Fig. 6E), and inferior colliculus (Fig. 6F), intensely labeled cell bodies and weak neuropil staining were observed.

Vestibular system: In the medial vestibular nucleus, intensely stained small neurons and strong neuropil staining were observed (Fig. 6G). In the lateral vestibular nucleus, although large-sized neurons exhibited strong BMP4-IR, neuropil staining was weak (Fig. 6H).

Visual system: In the superior colliculus, the superficial gray layer showed very intense BMP4-IR in the neuropil (Figs. 2H and 6I). Very strong BMP4-IR in neurons and the neuropil was also observed in the parabigeminal nucleus (Fig. 6J).

Other lower brain stem areas

Very strong cell body and neuropil staining were observed in the raphe pallidus (Fig. 6K). In the dorsal tegmental area, intense neuropil staining was observed, while neuropil staining in the caudal pontine reticular nucleus was weak (Fig. 6L). In the locus coeruleus, strong neuropil staining and moderate cell body staining were seen (Fig. 5J). In the pontine nucleus, strong neuropil and cell body staining was observed (Fig. 6M). Very intense neuropil and cell body staining was also seen in the area postrema (Fig. 2J). The inferior olive nucleus also showed intense BMP4-IR (Fig. 7C).

Cerebellum

In the cerebellum, the molecular layer showed very strong neuropil staining. In addition, dendrites of Purkinje neurons were also very intensely stained (Fig. 7A). In the Purkinje cell layer, cell bodies of Purkinje neurons showed very strong BMP4-IR (arrowheads in Fig. 7A). In addition, cell bodies of Bergmann glia seemed to be also stained. The granular layer exhibited a mosaic pattern. The cerebellar nuclei contained intensively labeled neurons (Fig. 7B).

Spinal cord

Intense BMP4-IR was observed in the gray matter, and the white matter also showed moderate staining (Fig. 7D). In the dorsal horn, very intense neuropil and cell body staining was observed in the layers I-II (Fig. 7E). In the ventral horn, large sized motor neurons exhibited very strong BMP4-IR both in the somata and dendrites (arrowheads in Fig. 7F).

Other areas

Intense BMP4-IR was also detected in the choroidal plexus (Fig. 7G) and in the subventricular zone (arrows in Fig. 7H).

BMP4 in astrocytes

To confirm whether the BMP4-IR postitive cells in the corpus callosum are astrocytes or oligodendrocytes. We performed double fluorescence immunohistochemistry using anti-GFAP antibody. Fig. 8 shows that BMP4-IR positive cells were simultaneously GFAP positive, indicating that astrocytes express BMP4.

DISCUSSION

To date, BMP4 expression in the adult brain has been investigated in the restricted regions (Fan et al., 2003; Charytonick et al., 2000; Peretto et al., 2002; Lim et al., 2000). In the present study, we first show that BMP4 is widely expressed throughout the adult CNS. In addition, besides intense BMP4 expression in neurons, we exhibit BMP4 expression in astrocytes. These results suggest that BMP4 is abundantly produced by neurons and astrocytes throughout the adult CNS. Since BMP4 receptors, such as BMPRIA and BMPRII, have been also reported to be abundantly expressed in the adult rat brain (Charytoniuk et al. 2000; Zhang et al. 1998), secreted BMP4 to the extracellular space might play pivotal roles via BMPRIA and BMPRII in the adult brain.

BMP4 in dendrites

Interestingly, we observed intense BMP4-IR in the dendrites of mitral cells and tufted cells in the olfactory bulb (Fig. 3B), the apical dendrites of pyramidal neurons in the piriform cortex (Fig. 3D), cerebral cortex (Fig. 3G), and hippocampus (Fig. 4B and C), and the dendrites of Purkinje cells (Fig. 7A). These cells are known to have high synaptic plasticity, and the involvement of BMPs and their receptors in the process of dendritic formation and maturation is well documented (Lein et al., 1995; Le Roux et al., 1999; Withers et al., 2000). Withers and colleagues working on cultures of hippocampal neurons showed that BMP7 acts as a growth factor selective for dendritic development. Addition of BMP7 to cultured hippocampal neurons results in a rapid and profound acceleration of dendritic growth and enhances synaptogenesis. Since the presence of BMPs and their receptors has been described in vivo in the adult hippocampus and olfactory bulb (Charytoniuk et al., 2000), regions where the dendritic arbor continues to be remodeled throughout life (Graziadei and Monti- Graziade, 1979; Stanfield and Trice, 1988), suggesting a role for BMPs in modulating this type of plasticity. In addition, enhancement of dendritic growth due to BMPs has

been demonstrated for sympathetic (Lein et al., 1995) and cerebral cortical neurons (Le Roux et al., 1999). Furthermore, Althini et al. (2004) have recently reported that BMP4 potentiates neurotrophin 3 and neurturin-induced neurite outgrowth of peripheral neurons from the E9 chicken embryo. Taken together, like other BMPs, BMP4 expressed in dendrites might also play a pivotal role in regulating dendritic branching and synapse formation.

BMP4 in the neuropil

In the present study, intense BMP4 expression was observed in the neuropil of the gray matter throughout the adult rat brain. Especially, this tendency was more prominent in the external plexiform layer of the olfactory bulb (Fig. 3B), and the molecular layer of the dentate gyrus (Fig. 4D). In the external plexiform layer, granule cells make synapses with the lateral dendrites of mitral and tufted cells. As neurogenesis of granule cells persists into adulthood (Kaplan and Hinds, 1977), newly synthesized neurons must make new synapses in this layer. Similarly, in the molecular layer of the dentate gyrus, perforant fibers from the entorhinal cortex make synapses with the dendrites of granule cells. Since granule cells in the dentate gyrus continue to be produced during adulthood (Gage, 2002), new synapses must be made in the molecular layer. These data suggest that BMP4 expressed in the neuropil of these regions might be needed to make an adequate environment, where newly produced neurons can elongate their axons and make new synaptic connections.

We also found intense BMP4-IR in the neuropil of the molecular layer of the cerebellum (Fig. 7A), the superficial layer of the dorsal cochlear nucleus (Fig. 6B), and the superficial layer of the superior colliculus (Fig. 6I). In the molecular layer of the cerebellum, parallel fibers originated from granule cells and climbing fibers originated from the inferior olive nucleus make synapses with the dendrites of Purkinje cells, where highly plastic phenomena, such as long-term depression (LTD) and long-term potentiation (LTP), are reported (Ito, 2001). The structure of the superficial layer of the

dorsal cochlear nucleus resembles that of the molecular layer of the cerebellum. The dorsal cochlear nucleus integrates acoustic information with multimodal sensory inputs from widespread areas of the brain. Multimodal inputs are brought to spiny dendrites of fusiform and cartwheel cells in the molecular layer by parallel fibers through synapses that are subject to LTP and LTD (Fujino and Oertel, 2003). In the superficial layer of the superior colliculus, also similar to the molecular layer of the cerebral cortex, many ascending dendrites of neurons situated in the deeper zones make synapses with marginal and horizontal cells, and this layer has also been reported to possess high plasticity (Giraldi-Guimaraes and Mendez-Oero, 2005). These data suggest that BMP4 in these regions might be involved in keeping plasticity by regulating important phenomena , such as LTP and LTD.

BMP4 in astrocytes

In the present study, we found that astrocytes express BMP4 protein. Peretto et al. (2002) have also reported BMP4 expression in astrocytes in the olfactory bulb, supporting our finding. What is the role of BMP4 secreted from astrocytes? In the adult CNS, Lim et al. (2000) have reported that in the adult subventricular zone (SVZ) BMP4 expressed in the SVZ astrocytes potently inhibits neurogenesis, and its antagonist noggin secreted from the ependymal cells makes a niche for adult neurogenesis. Thus, one possibility might be that, also in the other brain regions, BMP4 secreted from astrocytes control local microenvironmental conditions. Another possibility might be that BMP4 secreted from astrocytes affects astrocytes themselves. For example, BMP4 promotes astrogliogenesis and inhibits oligodendrocyte preprogenitors or precursors from becoming immature oligodendrocytes (Gross et al., 1996; Mabie et al., 1997). In addition, Gomes et al. (2003) have reported that transgenic overexpression of BMP4 increases astroglial and decreases oligodendroglial lineage commitment. These data raise the possibility that BMP4 signaling somehow controls the functions of astrocytes. Interestingly, Gomes et al. (2003) have shown that there was a

widespread increase in the number of GFAP positive astroctyes in BMP4 overexpressed transgenic mice, suggesting that BMP4 signaling also controls the level of GFAP expression. In the present study, we found intense BMP4-IR in astrocytes in the corps callosum and Bergmann glia in the cerebellum. Since both cell types are known to express high levels of GFAP protein, BMP4 might be involved in keeping GFAP expression in these regions.

Comparison with other studies

BMP4 expression in the adult brain has been also investigated in some publications (Fan et al., 2003; Charytonick et al., 2000; Peretto et al., 2002; Lim et al., 2000). Fan et al. (2003) have reported using cRNA in situ technique that BMP4 mRNA was expressed in the CA1-CA4, the hilus of the dentate gyrus, and the granular cell layer of the dentate gyrus. Although they did not clearly show the cell types of these BMP4 mRNA positive cells, this data is basically coincident with our data showing abundant BMP4 protein expression in the same areas. However, Peretto et al. have reported that BMP4-IR was detected in the most layers of the olfactory bulb until P14, however, in the adult only the subependymal layer exhibited BMP4-IR. This data does not fit with our data showing abundant BMP4-IR expression in the most layers of the adult olfactory bulb. This discrepancy would be difficult to explain, however, it might be originated from using different antibodies and immunostaining procedures. Further studies are still needed to clarify these kinds of discrepancies.

LITERATURE CITED

Althini S, Usoskin D, Kylberg A, Kaplan PL, Ebendal T. 2004. Blocked MAO kinase activity selectively enhances neurotrophic growth responses. Mol Cell Neurosci 25: 345-354.

Charytoniuk DA, Traiffort E, Pinard E, Issertial O, Seylaz J, Ruat M. 2000. Distribution of bone morphogenetic protein and bone morphogenetic protein receptor transcripts in the rodent nervous system and up-regulation of bone morphogenetic protein receptor type II in hippocampal dentate gyrus in a rat model of global cerebral ischemia. Neurosci 100: 33-43.

Cho KW, Blitz IL. 1998. BMPs, Smads and metaloproteases: extracellular and intracellular modes of negative regulation. Curr Opin Genet 8: 443-449.

Crossley PH, Martinez S, Ohkubo Y, Rubenstein JLR. 2001. Coordinate expression of FGF8, OTX2, BMP4, and SHH in the rostal prsencepahlon during development of the telencephalic and optic vesicles. Neurosci 108: 183-206.

Fan X, Xu H, Cai W, Yang Z, Zhang J. 2003. Spatial and temporal patterns of expression of Noggin and BMP4 in embryonic and postnatal rat hippocampus. Dev Brain Res 146: 51-58.

Fujino K, Oertel D. 2003, Bidirectional synaptic plasticity in the cerebellum-like mammalian dorsal cochlear nucleus. PNAS 100, 265-270.

Furuta Y, Pitson DW, Hogan BLM. 1997. Bone morphogenetic proteins (BMPs) as regulators of dorsal forebrain development. Development 124: 2203-2212.

Gage FH 2002. Neurogenesis in the adult brain. J Neurosci 22: 612-613.

Gomes WA, Mehler MF, Kessler JA. 2003. Transgenic overexpression of BMP4 increases astroglial and decreases oligodendroglial lineage commitment. Dev Biol 255: 164-177.

Gradiadei PPC, Monti-Gradiadei GA. 1979. Neurogenesis and neuron regeneration in the olfactory system of mammals. I. Morphological aspects of differentiation and structural organization of the olfactory neurons. J Nerurocytol 8: 1-18.

Giraldi-Guimaraes A, Mendez-Otero R. 2005. Induction of the candidate-plasticity NGFI-A protein in the adult rat superior colliclulus after visual stimulation. Mol Brain Res 133: 242-252.

Graham A, Francis-West P, Brickell P, Lumsden A. 1994. The signaling molecule BMP4 mediates apoptosis in the rhombencephalic neural crest. Nature 372: 684-686.

Gross RE, Mehler MF, Mabie PC, Zhang Z, Santschi L, Kessler JA. 1996. Bone morphogenetic proteins promote astroglial lineage commitment by mammalian subventricular zone progenitor cells. Neuron 17: 595-606.

Harland R. 2000. Neural induction. Curr Opin Genet Dev 10: 357-362.

Hogan BLM. 1996. Bone morphogenetic proteins: multifunctional regulators of vertebrate development. Genes Dev 10: 1580-1584.

Ito M. 2001. Cerebellar long-term depression: characterization, signal trasnsduction and functional roles. Physiol Rev 81: 1143-1195.

Jones CM, Lyons KM, Hogan BL. 1991. Involvement of bone morphogenetic protein-4 (BMP-4) and Vgr-1 in morphogenesis and

neurogenesis in the mouse. Development 111: 531-542.

Kaplan MS, Hinds JW. 1977. Neurogenesis in the adult rat, electron microscopic analysis of light radiographs. Science 197: 1092-1094.

Kulessa H, Turk G, Hogan BL. 2000. Inhibition of Bmp signaling affects growth and differentiation in the anagen hair follicle. EMBO J 19: 6664-6674.

Lein P, Johnson M, Guo X, Reuger D, Higgins D. 1995. Osteogenic protein-1 induces dendritic growth in rat sympathetic neurons. Neuron 15: 597-605.

Le Roux P, Behar S, Higgins D, Charette M. 1999. OP1 enhances dendritic growth from cerebral cortical neurons in vitro. Exp Neurol 160: 151-163.

Lim DA, Tramontin AD, Trevejo JM, Herrera DG, Gracia-Verdugo JM, Alvarez-Buylla A. 2000. Noggin antagonizes BMP singaling to create a niche for adult nuerogenesis. Neuron 28: 713-726.

Mabie PC, Mehler MF, Kessler JA. 1999. Multiple roles of bone morphogenetic protein signaling in the regulation of cortical cell number and phenotype. J Neurosci 19: 7077-7088.

McMahon JA, Takada S, Zimmerman LB, Fan CM, Harland RM, McMahon AP. 1998. Noggin-mediated antagonism of BMP signaling is required for growth and patterning of the neural tube and somite. Genes Dev 12: 1438-1452.

Peretto P, Cummings D, Modena C, Behrens M, Venkatraman G, Fasolo A, Margolis FL. 2002. BMP mRNA and protein expression in the developing mouse olfactory system. J Comp Neurol 451: 267-278.

Sasai Y, De Robertis EM. 1997. Ectodermal patterning in vertebrate embryos. Dev Biol 182: 5-20.

Stanfield BB, Trice JE. 1988. Evidence that granule cells generated in the dentate gyrus of adult rats extend axonal projections. Exp Brain Res 72: 399-406.

Ueki T, Tanaka M, Yamashita K, Mikawa S, Qiu ZF, Maragakis NJ, Hevner RF, Miura N, Sugimura H, Sato K. 2003. A novel secretory factor, neurogenesin-1, provides neurogenic environmental cues for neural stem cells in the adult hippocampus. J Neurosci 23: 11732-11740.

Watt FM, Hogan BL. 2000. Out of Eden: stem cells and their niches. Science 287: 1427-1430.

Withers GS, Higgins D, Charette M, Banker G. 2000. Bone morphognenetic protein-7 enhances dendritic growth and receptivity to innervation in cultured hippocampal neurons. Eur J Neurosci 9: 683-691.

Wozney JM. 1989. Bone morphogenetic proteins. Prog Growth Factor Res 1: 267-280.

Zhang D, Mehler MF, Song Q, Kessler JA. 1998. Development of bone morphogenetic protein receptors in the nervous system and possible roles in regulating trkC expression. J. Neurosci 18: 3314-3326.

Figure legends

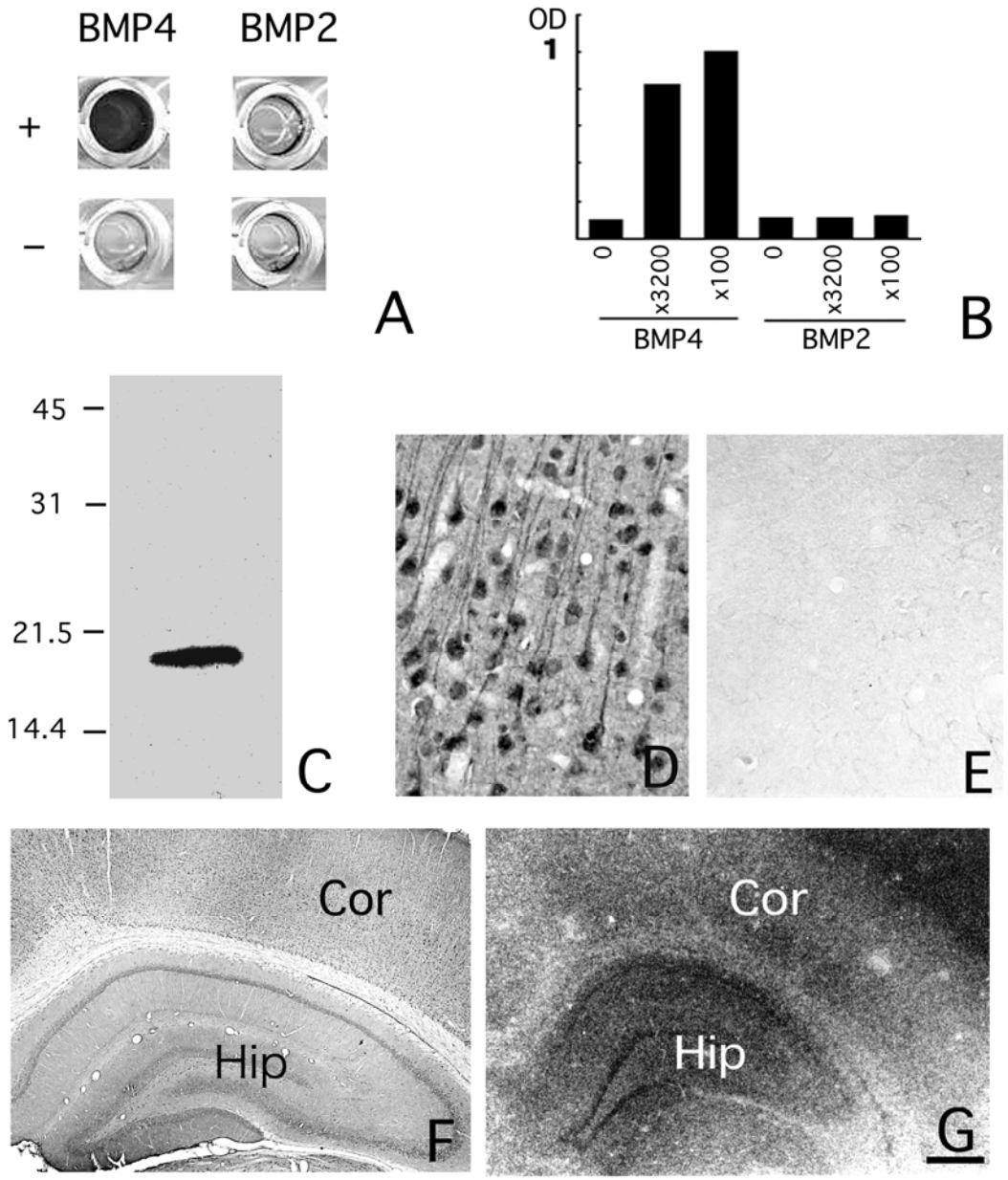

Fig. 1. Specificity of anti-BMP4 antibody. Wells added with NCL-BMP4 antibody (+) show intense ELISA reaction only when coated by BMP4 protein, but not BMP2 protein. Wells without the first antibody (-) show no ELISA reaction against both proteins (**A**). NCL-BMP4 specifically recognizes only BMP4 protein in a dose-dependent manner (**B**). Western blot analysis using NCL-BMP4 shows a single band of about 19 Kd (**C**). Photomicrographs of pre-absorption tests; control (**D**), pre-absorbed (**E**). Note that immunoreactivities in the layer V of the cortex are completely abolished by pre-absorption tests. Comparison between BMP4 protein expression (F) and BMP4 mRNA expression (G). Note that in both procedures, intense reactivities or signals are observed in the cerebral cortex and hippocampus. Cor, cortex; Hip, hippocampus. Scale bar, 100 μm (D and E), 1 mm (F and G).

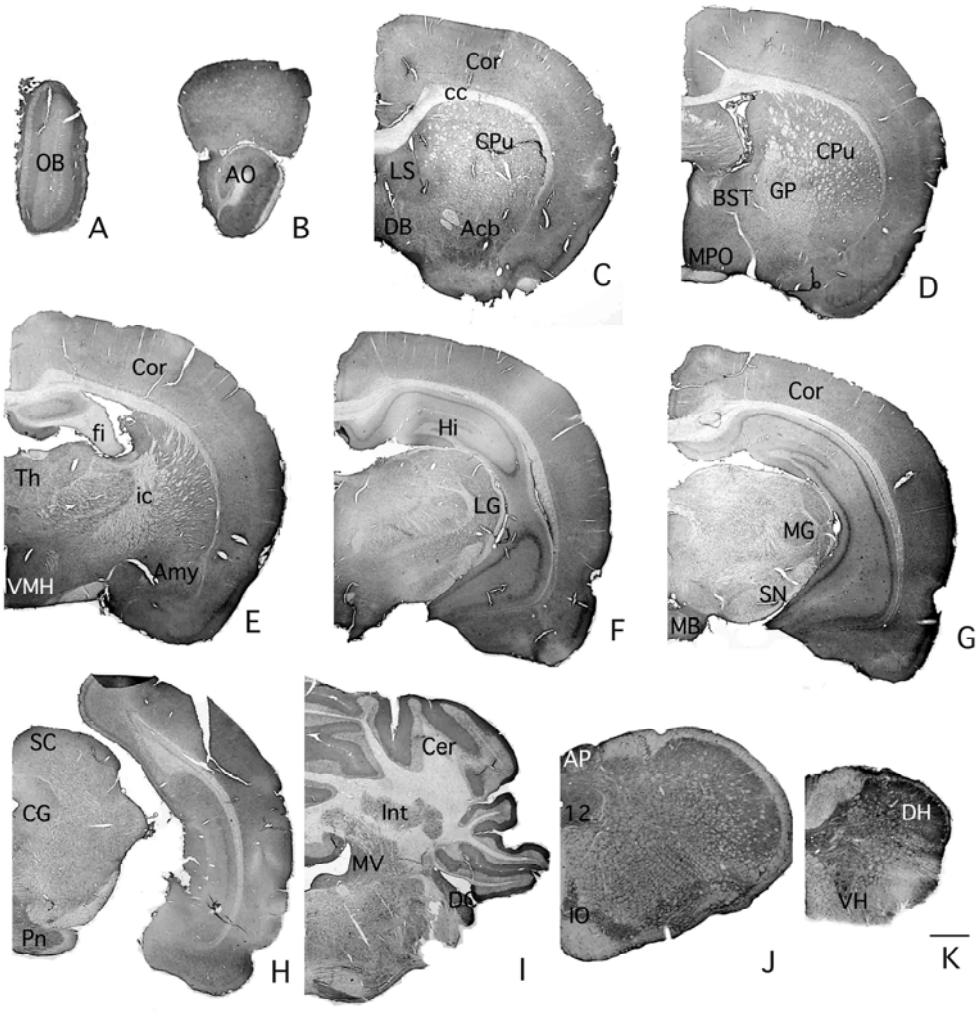

Fig. 2. BMP4 expression in the whole rat brain. 12, hypoglossal nucleus; Acb, accumbens nucleus; Amy, amygdala; AO, anterior olfactory nucleus; AP, area postrema; BST, bed nucleus of the stria terminalis; cc, corpus callosum; Cer, cerebellum; CG, central gray; Cor, cerebral cortex; CPu, caudate putamen; DB, diagonal band; DC, dorsal cochlear nucleus; DH, dorsal horn; fi, fimbria of the hippocampus; GP, globus pallidus; Hi, hippocampus; ic, internal capsule; IN, interposed cerebellar nucleus; IO, inferior olive; LG, lateral geniculate nucleus; LS, lateral septum; MB, mammillary body; MG, medial geniculate nucleus; MPO, medial preoptic nucleus; MV, medial vestibular neucleus; OB, olfactory bulb; Pn, pontine nucleus; SC, superior colliculus; SN, substantia nigra; Sp5, spinal trigeminal nucleus; VH, ventral horn; VMH, ventromedial hypothalamic nucleus. Scale bar, 2 mm (A, B and J), 3 mm (C-I), 1 mm (K).

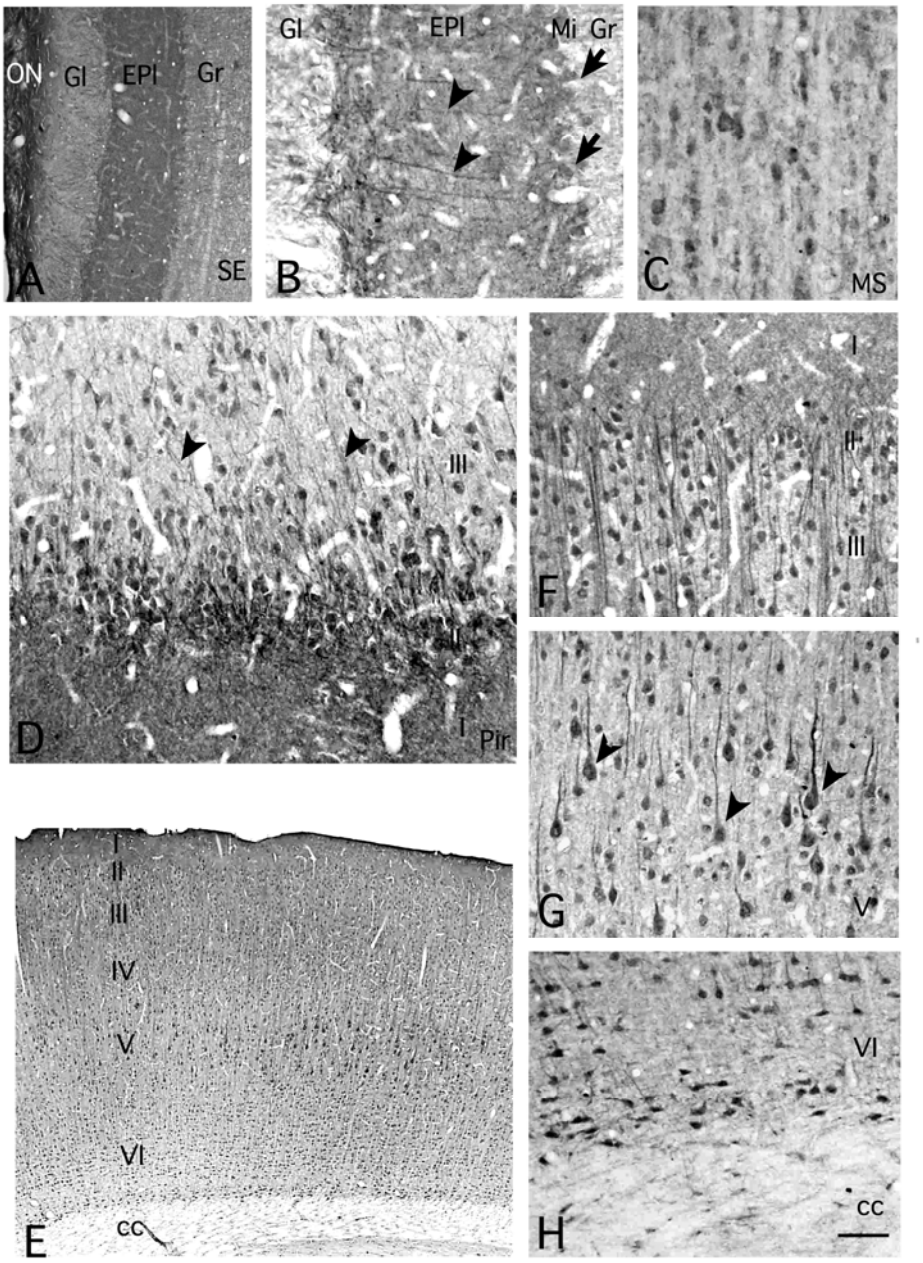

Fig. 3. BMP4 expression in the olfactory bulb (**A, B**), medial septal nucleus (**C**), piriform cortex (**D**), and cerebral cortex (**E-H**). I-VI, layers I-VI; cc, corpus callosum; EPl, external plexiform layer; Gl, glomerular layer; Gr, granular layer; Mi, mitral cell layer; MS, medial septal nucleus; ON, olfactory nerve layer; Pir, piriform cortex; SE, subependymal layer. Scale bar, 1 mm (A), 100 μm (B-D and F-H), 400 μm (E).

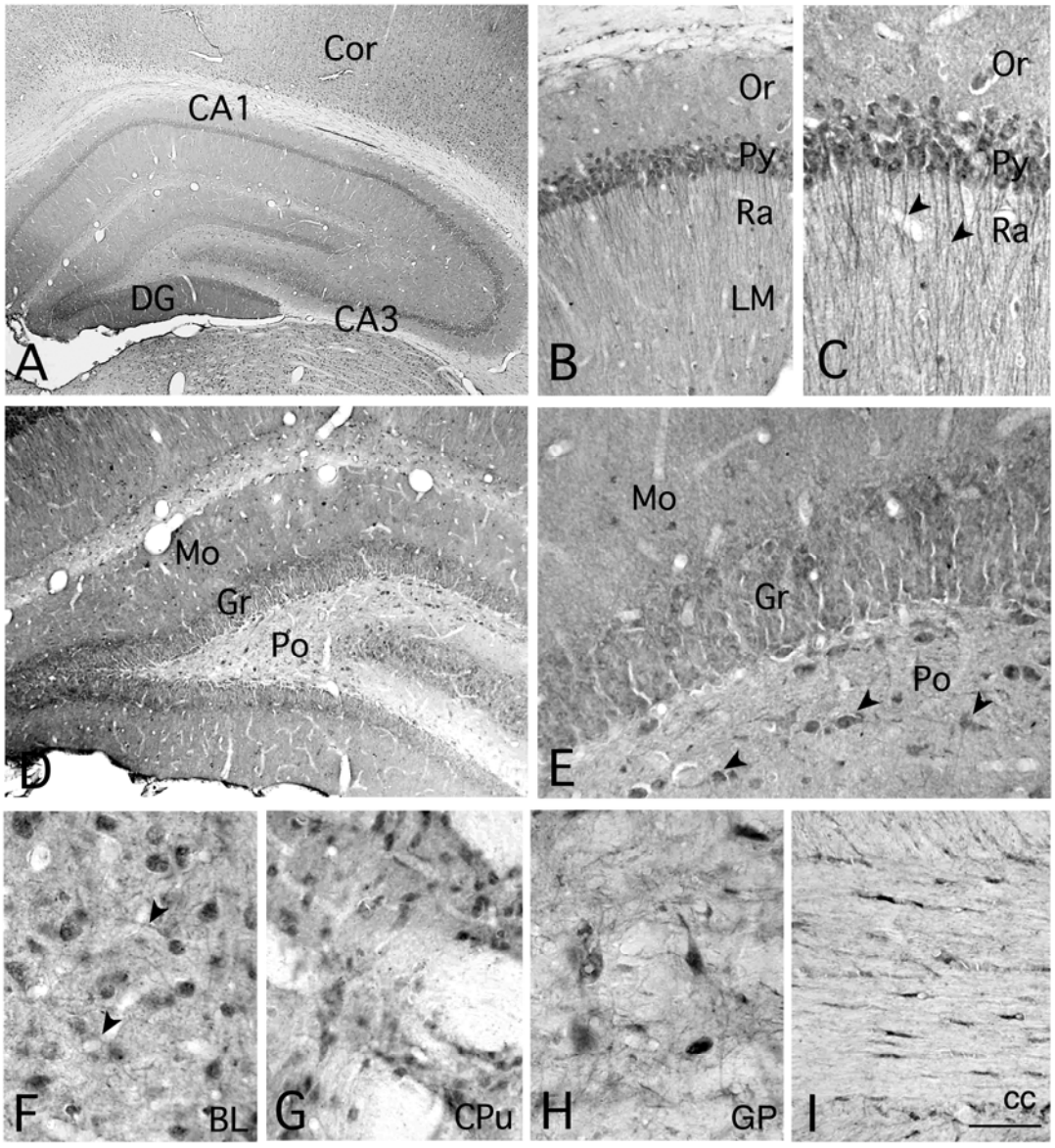

Fig. 4. BMP4 expression in the hippocampus (**A-E**), basolateral amygdaloid nucleus (**F**), caudate putamen (**G**), globus pallidus (**H**) and in the corpus callosum (**I**). BL, basolateral amygdaloid nucleus; CA1, 3, fields CA1, 3 of Ammon's horn; cc, corpus callosum; Cor, cerebral cortex; CPu, caudate putamen; DG, dentate gyrus; GP, globus pallidus; Gr, granular layer; LHb, lateral habenular nucleus; LM, stratum lacnosum-moleculare; Mo, stratum moleculare; Or, stratum oriens; Po, polymorphological layer; Py, stratum pyramidale; Ra, stratum radiatum. Scale bar, 1 mm (A), 200 μm (B), 100 μm (C, E, F-I), 400 μm (D).

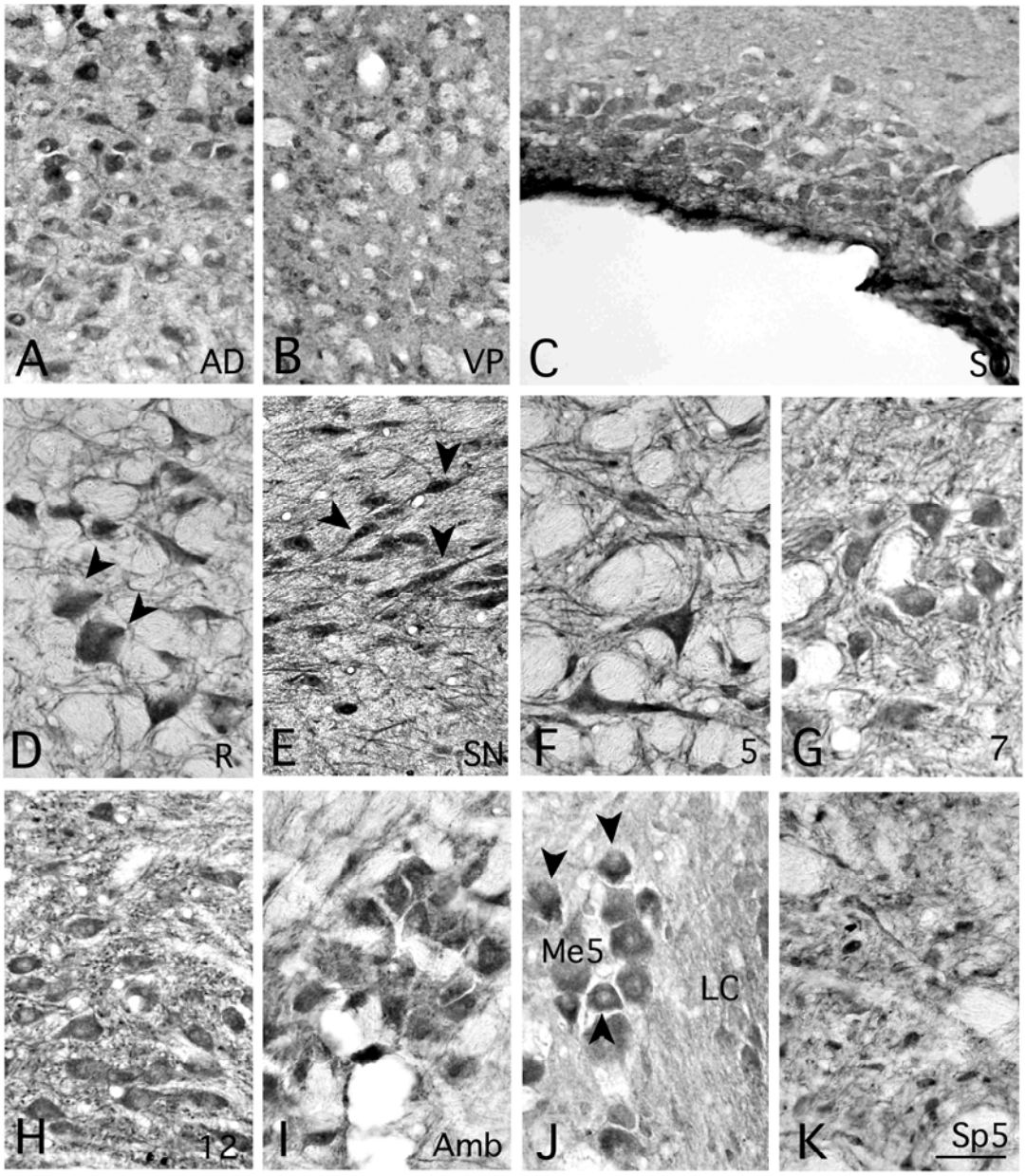

Fig. 5. BMP4 expression in the anterodorsal thalamic nucleus (**A**), ventroposterior thalamic nucleus (**B**), supraoptic nucleus (**C**), red nucleus (**D**), substantia nigra (**E**), trigeminal motor nucleus (**F**), facial nucleus (**G**), hypoglossal nucleus (**H**), ambiguous nucleus (**I**), mesencephalic trigeminal nucleus (**J**), spinal trigmeninal nucleus (**K**). 5, motor trigeminal nucleus; 7, facial nucleus; 12, hypoglossal nucleus; Amb, ambiguous nucleus; AD, anterodorsal thalamic nucleus; LC, locus coeruleus; Me5, mesencephalic trigeminal nucleus; R, red nucleus; SN, substantia nigra; SO, supraoptic nucleus; Sp5, spinal trigeminal nucleus; VP, ventroposterior thalamic nucleus. Scale bar, 100 μm.

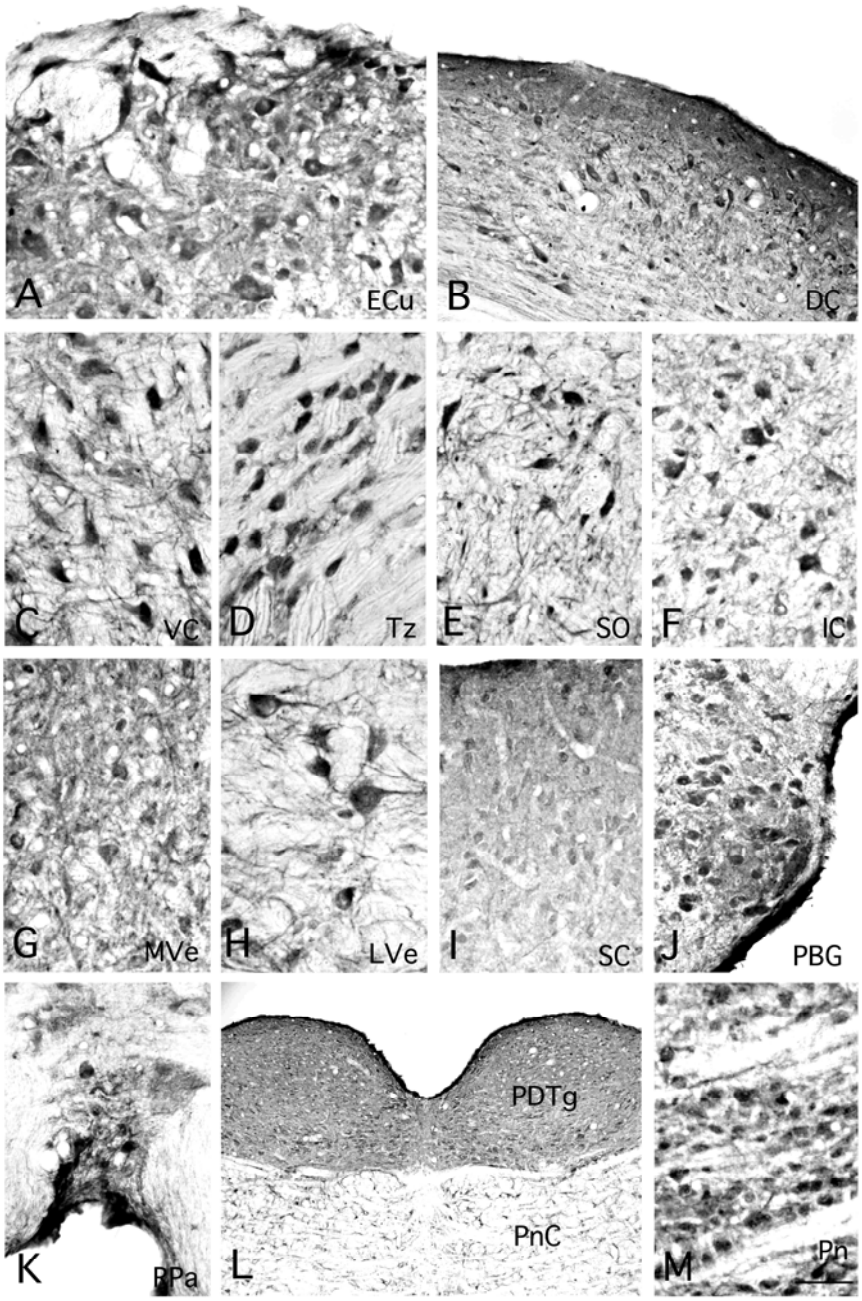

Fig. 6. BMP4 expression in the external cuneate nucleus (**A**), dorsal cochlear nucleus (**B**), ventral cochlear nucleus (**C**), trapezoid nucleus (**D**), superior olive (**E**), inferior colliculus (**F**), medial vestibular nucleus (**G**), lateral vestibular nucleus (**H**), superior colliculus (**I**), parabigeminal nucleus (**J**), raphe pallidus (**K**), posterodorsal tegmental nucleus (**L**), and pontine nucleus (**M**). DC, dorsal cochlear nucleus; ECu, external cuneate nucleus; IC, inferior colliculus; LVe, lateral vestibular nucleus; MVe, medial vestibular nucleus; PBG, parabigeminal nucleus; PDTg, posterodorsal tegmental nucleus; Pn, pontine nucleus; PnC, caudal pontine reticular nucleus; RPa, raphe pallidus; SC, superior colliculus; SO, superior olive; Tz, trapezoid nucleus; VC, ventral cochlear nucleus. Scale bar, 100 μm.

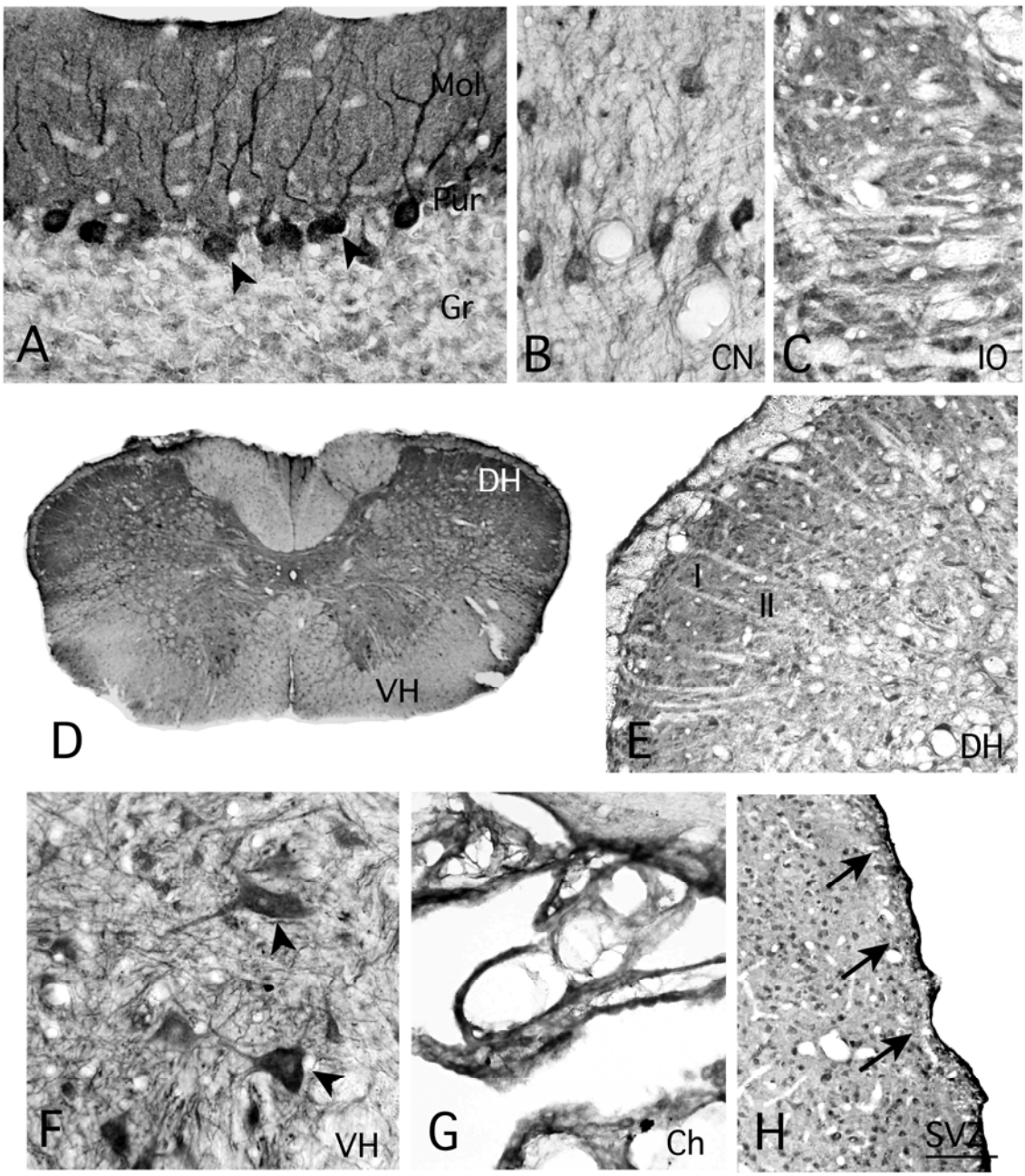

Fig. 7. BMP4 expression in the cerebellar cortex (**A**), cerebellar nucleus (**B**), inferior olive (**C**), spinal cord (**D-F**), choroidal plexus (**G**), subventircular zone (**H**). II, the layer II of the spinal cord; ch, choroidal plexus; CN, cerebellar nucleus; DH, dorsal horn; Gr, granular layer; IO, inferior olive; Mol, molecular layer; Pur, Purkinje cell layer; SVZ, subventricular zone; VH, ventral horn. Scale bar, 100 μm (A-C and E-H), 1 mm (D).

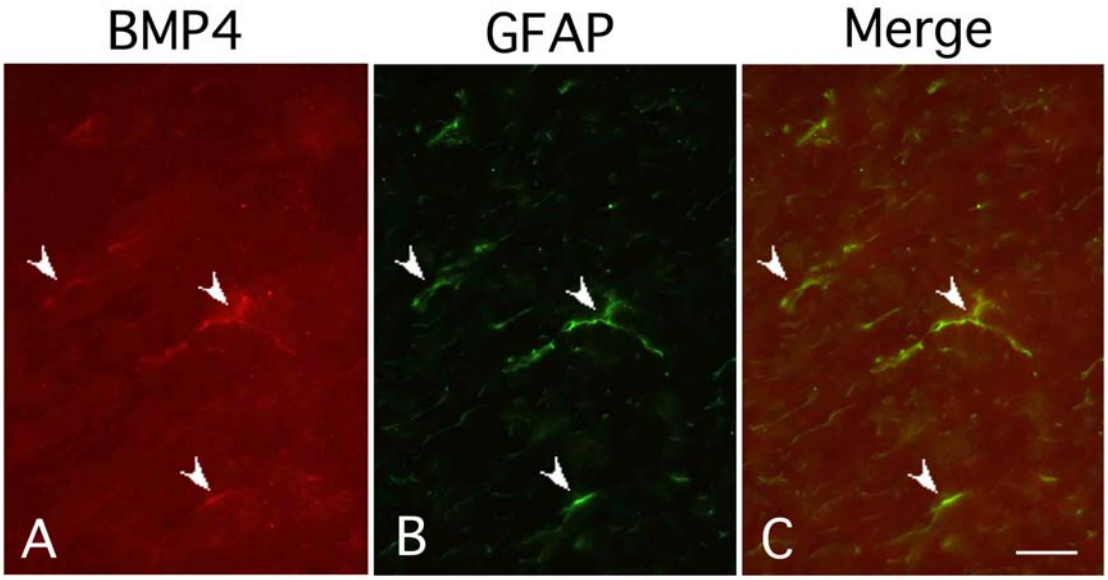

Fig. 8. Double-staining study showing that BMP4-IR postive cells in the corpus callosum (**A**) are also positive for GFAP (**B**) in a merged photomicrograph (**C**). Scale bar, 20 μm.

Table 1. Distribution and intensity of BMP4-IR in the rat nervous system

Area and cell type	Cell body	Neuropil
I. Telencephalon		
Olfactory bulb		
External plexiform layer	+++	++++
Mitral layer	++++	++
Granular layer	++	++
Cerebral cortex		
Layer I	+++	+++ +
Layer V	++++	++
Hippocampal formation		
Ammon's horn	++++	+++
Dentate gyrus	+++	++++
Amygdala		
Basolateral nucleus	+++	++
Basal ganglia		
Caudate putamen	++++	+++
Globus pallidus	+++	+
II. Diencephalon		
Thalamus		
Anterodorsal nucleus	++++	++
Ventroposterior nucleus	+++	++
Hypothalamus		
Supraoptic nucleus	+++	+++
III. Midbrain		
Red nucleus	+++	+
Substantia nigra	+++	++
IV. Pons and Medulla		
Motor system		
Motor trigeminal nucleus	++++	++
Facial nucleus	++++	++
Hypoglossal nucleus	++++	++
General somatosensory system		
Trigeminal mesencephalic nucleus	+++	++
Ttrigeminal spinal nucleus	+++	++
External cunate nucleus	++++	+++
Auditory system		
Dorsal cochlear nucleus	++++	++++
Ventral cochlear nucleus	+++	+
Vestibular system		
Medial vestibular nucleus	+++	+++
Lateral vestibular nucleus	++++	+
Visual system		
Superior colliculus	+++	++++
Parabigeminal nucleus	++++	++++
Raphe pallidus	++++	++++
Locus caeruleus	++	+++
Pontine nuclei	+++	+++
V. Cerebellum		
Cortex		
Molecular layer	++++	++++
Purkinje cell layer	++++	++
Granule cell layer	+	+
Cerebellar nuclei	+++	+
VI. Spinal cord		
Dorsal horn	++++	+++
Ventral horn	++++	++

Relative intensities were estimated by visual comparison of immunostained slides: +, low; ++, moderate; +++, strong; ++++, very strong.